Predictive Analysis of Wildfire Smoke-Induced Wiggle Effect on Low-Inertia Trending Power Grids

Amjad Jebril Ali, *Member, IEEE*, Long Zhao, Mohammad Heidari Kapourchali, *Member, IEEE*, and Wei-Jen Lee, *Life Fellow, IEEE*

Abstract*—By the end of 2021, the United States had installed a 92.5 gigawatts of solar systems. Simultaneously, the rise of inverter-based resources (IBRs) has resulted in a noticeable decline in power grid inertia, which poses a risk to frequency stability in power systems. With the increasing prevalence of wildfires worldwide, it is crucial to examine the impact of wildfire smoke on solar systems and its implications for power grid operations. This study explores the oscillatory power output of PV systems named as "Wiggle Effect," a phenomenon observed in PV systems during days affected by wildfire smoke. Distinctive from impact of cloud cover on PV systems, wildfire smoke covers much more landmass and can cause regional impacts on power grids. Additionally, wildfire smoke lasts for a longer time. Therefore, this study investigates the oscillatory patterns of PV power output, which have the potential to jeopardize the frequency stability of the power grid due to sudden fluctuations in power generation. The study investigates this effect and its impact on power system stability, focusing on power systems characterized by low inertia trends. Understanding the influence of wildfire smoke on power grid operations is essential for system operators to develop effective frequency control practices. By gaining insights into the Wiggle Effect, operators can enhance the stability and reliability of power grid operations, mitigating the risks associated with wildfire smoke episodes. The study's findings contribute to a comprehensive understanding of this issue, facilitating informed decision-making in managing power systems in the presence of wildfire smoke.

***Index Terms*—Frequency response, frequency stability, low inertia, power system stability, PV systems, stability analysis, wiggle effect, wildfire smoke.**

Manuscript received 13 June 2023; revised 15 October 2023; accepted 13 November 2023. Date of publication 13 December 2023; date of current version 21 March 2024. This work was supported in part by the U.S. National Science Foundation under Grants RISE-2220624 and RISE-2022705. Paper 2023-PSPC-0865.R1, presented at the 2023 IEEE/IAS 59th Industrial and Commercial Power Systems Technical Conference, Las Vegas, NV, USA, May 21–25, and approved for publication in the IEEE TRANSACTIONS ON INDUSTRY APPLICATIONS by the Power Systems Protection Committee of the IEEE Industry Applications Society [DOI: 10.1109/ICPS57144.2023.10142096]. *(Corresponding author: Long Zhao.)*

Amjad Jebril Ali and Long Zhao are with the Department of Electrical Engineering and Computer Science, South Dakota School of Mines and Technology, Rapid City, SD 57701 USA (e-mail: amjed.jebril@gmail.com; long.zhao@sdsmt.edu).

Mohammad Heidari Kapourchali is with the Department of Electrical Engineering, University of Alaska Anchorage, Anchorage, AK 99508 USA (e-mail: mhkapourchali@alaska.edu).

Wei-Jen Lee is with the Electrical Engineering Department, University of Texas at Arlington, Arlington, TX 76019 USA (e-mail: wlee@uta.edu).

Color versions of one or more figures in this article are available at https://doi.org/10.1109/TIA.2023.3342767.

Digital Object Identifier 10.1109/TIA.2023.3342767

I. Introduction

In recent years, there has been a significant increase in the frequency and severity of wildfires globally, primarily attributable to extreme drought and high temperatures. Notable records of burned acreage have been reported in various countries worldwide. For instance, in 2020, more than 60 hectares of land were burned in Australia [1], while within the European Union countries, between 1.2 million acres and 1.6 million acres were burned, as reported by the European Forest Fire Information System (EFFIS) in October 2021 [2]. Similarly, the Canadian Interagency Forest Fire Centre (CIFFC) documented 6317 wildfires that burned approximately 10.34 million acres in Canada as of September 15, 2021 [3]. In the United States, an annual average of 70600 wildfires burned an average of 7.0 million acres since 2000 [4]. The U.S. National Interagency Coordination Center reported 58985 and 58950 wildfires in 2021 and 2020, respectively [5]. In 2022, the state of Alaska declared a state of emergency due to wildfires, with over 2 million acres burned by July 2nd [6], [7].

To address the crisis of global warming, a significant solution lies in renewable energy generation. In 2020, renewable energy set a new record in terms of new power capacity and was the sole source of electricity generation that experienced net expansion [8]. The International Energy Agency (IEA) reported that nearly 290 gigawatts (GW) of new renewable power capacity were commissioned in 2021, with solar photovoltaic (PV) systems accounting for over half of this expansion [9]. The global installed capacity of PV systems has been growing exponentially each year, facilitated by declining prices and maturing technology [10], [11]. Between 2010 and 2021, global PV capacity additions increased from 17 GWdc to 172 GWdc, reaching a cumulative installed capacity of 939 GWdc by the end of 2021 [11]. Furthermore, governmental policies are supporting this transition, as exemplified by the approval of the Federal Energy Regulatory Commission (FERC) Order 2222, enabling distributed energy resources (DERs) to participate in wholesale electricity markets through aggregation [12]. Moreover, the U.S. government aims to achieve 100 percent carbon pollution-free electricity by 2035 [13] and establish a net-zero economy no later than 2050 [14].

The proliferation of renewable energy sources (RESs), specifically inverter-based resources (IBRs), poses challenges to the stability of power grids. Unlike conventional power plants

(CPPs), IBRs lack sufficient inertia, which is the capacity of a power system to resist frequency changes. Inertia is determined by the kinetic energy stored in rotating masses of synchronous machines. Therefore, the increasing integration of IBRs such as photovoltaic (PV) generation in the grid introduces difficulties in maintaining power system stability due to the higher rate of change of frequency (ROCOF) associated with high IBR penetration.

Numerous studies have investigated the stability of low-inertia power grids. One study [17] examines the challenges posed by inertia in power systems with a high penetration of RESs and explores the feasibility of implementing new technologies in low-inertia systems. Another study [18] presents a method for dynamic event data-based stability risk assessment, while a different approach to analyzing small-signal stability for large-scale power systems is introduced in another study [19]. The impact of societal events on frequency stability, considering the increasing use of LED TVs and the trend towards low-inertia power grids, is investigated in yet another study [20]. Frequency regulation challenges arising from the integration of renewable energy units into power systems are discussed in a study that proposes a strategy to mitigate their impact on frequency stability [21]. Microgrid frequency regulation is addressed in several studies. One study [22] presents a novel frequency regulation method utilizing ultracapacitors and batteries in microgrids, demonstrating the effectiveness of the proposed frequency controller for primary frequency regulation. Another study [23] addresses voltage and frequency fluctuations associated with renewable energy integration and introduces various control technologies to overcome these challenges. Additionally, a study [24] focuses on wind and PV power plants' frequency control, including inertia control and governor control, within the U.S. Eastern and Texas Interconnections, revealing that synthetic inertia and governor control can mitigate the adverse effects of increasing RESs in both interconnections. Lastly, a study [25] develops a controller for inverters to enhance the frequency response of microgrids under disturbances.

Increasing the use of IBRs results in a low inertia trend and poses challenges for power grids with a high penetration of PV systems. These challenges are further compounded by the rising frequency of wildfires [27]. Wildfire emissions consist of various chemically reactive substances, including short-lived trace gases, particulate matter, and aerosols [28], [29], [30]. The smoke generated by wildfires travels long distances, covering extensive geographical areas. When this smoke reaches the atmosphere, it obstructs solar radiation, leading to a significant reduction in PV power generation. Numerous studies and reports have examined the impact of wildfire smoke on solar generation from different perspectives. For example, in September 2020, California experienced a decline of nearly 30% in average solar-powered electricity generation due to the widespread presence of wildfire smoke [31]. Despite a 5.3% increase in installed solar generating capacity since September 2019, solar generation in California during September 2020 was 13.4% lower compared to the previous year [31]. Researchers in [32] demonstrated that PV productivity reduction due to wildfire smoke ranged from 7% to 27%. In another study [33], a new index parameter was developed to quantify the impact of wildfire smoke on PV systems. The researchers investigated the PV power output in the Black Hills area of South Dakota during two wildfire events, and their findings revealed a significant reduction in PV power output caused by the smoke. Similarly, studies [34], [35], [36], [37] have explored the decrease in power generation of PV systems resulting from wildfire smoke. Several models have been developed to estimate this reduction in solar generation. In the latest report from NREL [38], the impact of wildfire smoke on grid stability is emphasized. The report underscores the importance of swiftly activating operating reserves when there's an abrupt drop in available solar radiation. These reserves are vital for preserving the balance between system supply and demand and for reestablishing stability following disruptions.

This paper investigates the impact of regional wildfire smoke on a 3-kW rooftop grid-tied PV system during smoky days in September 2022. A distinct power generation phenomenon, referred to as the "Wiggle Effect," is identified and thoroughly examined. The primary contributions of this study can be outlined as follows:

- Observation and Introduction of the "Wiggle Effect": The study identifies a unique phenomenon called the "Wiggle Effect" that occurs because of wildfire smoke on PV power output. This effect is thoroughly described and introduced in the paper.
- Differentiation of Wildfire Smoke and Cloud Impacts: The paper discusses and differentiates the impacts of both wildfire smoke and cloud cover on PV power output. By distinguishing between these two factors, a clearer understanding of their individual contributions to power generation variability is achieved.
- Investigation of Frequency Stability Considering the Wiggle Effect: The study explores the implications of the Wiggle Effect on frequency stability in power systems, particularly in the context of the United States. By considering this phenomenon, the paper contributes to the understanding of how PV power output variations induced by wildfire smoke can impact the stability of the grid's frequency.
- Predictive Assessment of the Wiggle Effect's Risk: Furthermore, this paper provides a predictive assessment of the potential risk posed by the Wiggle Effect on frequency stability. Considering the increasing capacity of PV installations and the low-inertia trend observed in power grids, the study offers insights into the future challenges associated with this phenomenon and its potential impact on the stability of power systems.

The remainder of the paper is organized as follows: Section II provides a detailed observation and analysis of the Wiggle Effect on PV power output. Section III presents an analysis of frequency stability taking into account the impact of the Wiggle Effect. In Section IV, a predictive analysis of frequency stability is conducted, considering the potential risks associated with the Wiggle Effect, the increasing capacity of PV installations, and the low-inertia trend observed in power grids. Finally, Section V summarizes the conclusions drawn from this study.

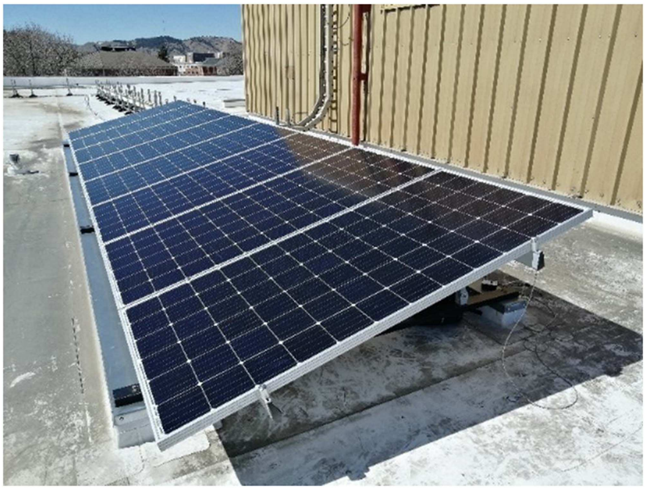

Fig. 1. 3-kW grid-tied PV system on campus.

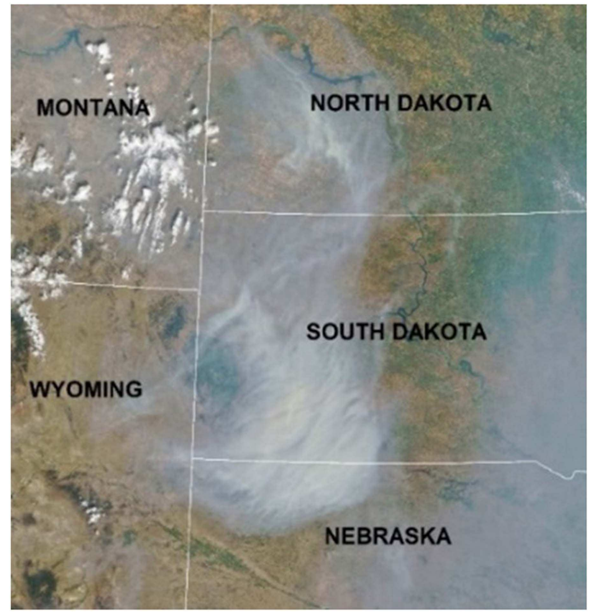

Fig. 2. NASA satellite image on September 7, 2022 [39].

II. Wiggle Effect Observation and Analysis

A. Research Facilities and Wildfire Events

In this study, a 3-kW rooftop grid-tied solar system comprising eight monocrystalline PV panels is installed at the South Dakota Mines Campus, as depicted in Fig. 1. The campus is geographically located at latitude 44.073922 and longitude −103.204919, with an elevation of 976 meters above sea level. The PV system is positioned with an azimuth of 215° and a tilt angle of 16°.

To gather data for analysis, a comprehensive monitoring system is implemented. This system records the PV power output at a resolution of 5 minutes and uploads the data to a cloud server at 15-minute intervals. Additionally, a scientific weather station is installed near the solar system. This weather station continuously provides real-time meteorological data at 15-minute intervals, including temperature, wind speed, humidity percentage, parametric pressure, global horizontal irradiance (GHI) at the horizontal plane, and barometric pressure. These measurements offer valuable insights into the environmental conditions surrounding the PV system and enable a thorough investigation of the system's performance.

During the period from September 4, 2022, to September 12, 2022, a widespread regional wildfire occurred across multiple states. The National Interagency Fire Center (NIFC) reported that, as of September 9, a total of 96 large fires were active, encompassing an area of 690000 acres (equivalent to approximately 2800 square kilometers) in eight states [39]. The majority of these fires were concentrated in the Northern Rockies, the Great Basin, and the Pacific Northwest regions, with 37 fires burning in Idaho, 22 in Montana, 12 in Oregon, 12 in Washington, and 10 in California. Fig. 2 displays an image captured by NASA's Terra satellite, which depicts the smoke emanating from the western fires and spreading over the Black Hills and northern plains on September 7, 2022 [39]. These figures clearly demonstrate that the South Dakota Mines campus remained under the influence of the wildfire smoke for several days.

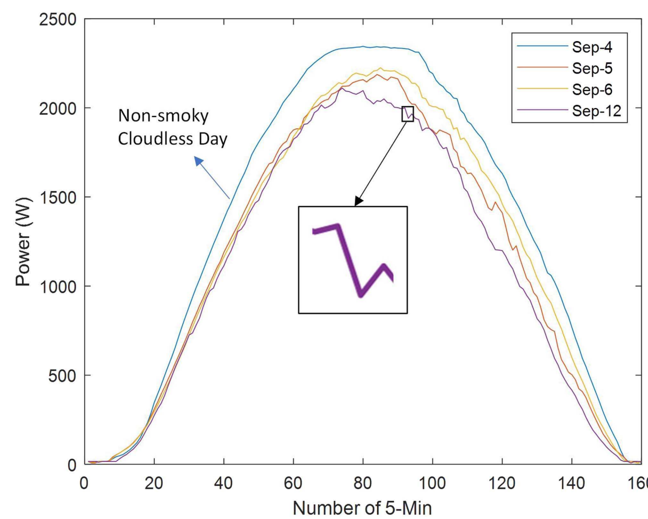

Fig. 3. 3-kW PV power output with 5-minute data.

B. Wiggle Effect Observation

This study utilizes the 5-minute power output data of a 3-kW rooftop grid-tied solar system. To mitigate the influence of clouds on PV generation, days characterized by cloudy and partially cloudy conditions during the period from September 4 to September 12 are excluded from the analysis.

During the periods affected by wildfire smoke, in addition to the overall reduction in power generation, a distinct power generation deviation, referred to as the "Wiggle Effect" in this study, is observed in the PV generation profiles, as depicted in Fig. 3. A comparison of the 5-minute PV generation curve on a non-smoky cloudless day (September 4th) with those on smoky days (September 5th, 6th, and 12th) reveals a much smoother

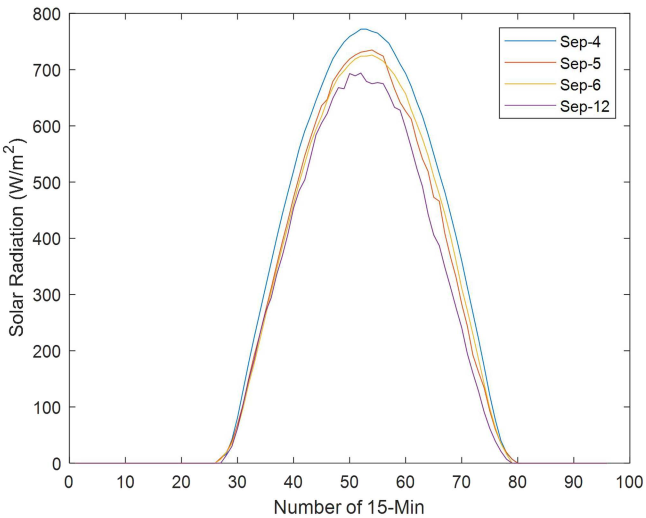

Fig. 4. Solar radiation curves with 15-minute data.

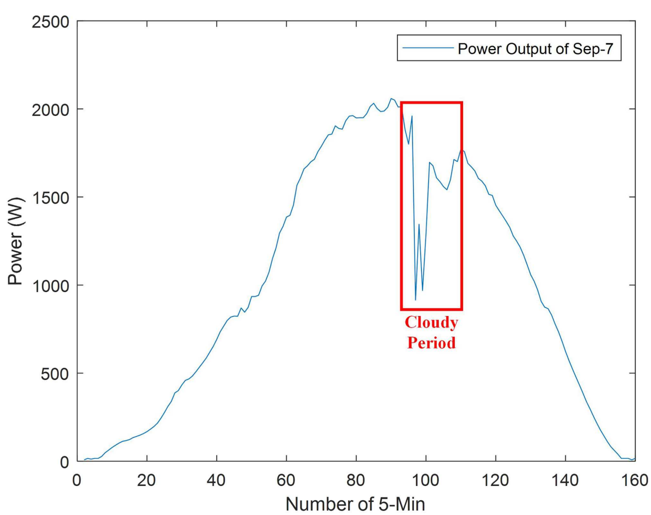

Fig. 5. 3-kW PV generation curve of a smoky and partial cloudy day.

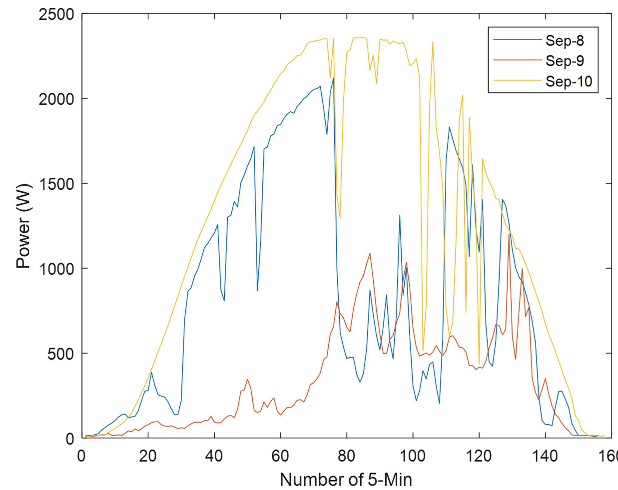

Fig. 6. 3-kW PV generation curves of cloudy and partial cloudy days.

pattern in the former. An example of the Wiggle Effect, characterized by a section of "Zigzag" power output on September 12th, is highlighted to illustrate the impact of wildfire smoke on solar power output. Additionally, Fig. 4 presents the 15-minute solar radiation data collected by the weather station for each day, demonstrating that the Wiggle Effect can still be observed based on solar radiation data during smoky days. However, due to the lower resolution of solar radiation data, the wiggle effect is not as pronounced as in the 5-minute power output data of the PV generation curves. This observation highlights the rapid nature of the Wiggle Effect, which can lead to swift deviations in power generation for power grids with a high penetration of PV systems.

To differentiate the Wiggle Effect from cloud impacts on PV systems, Fig. 5 illustrates the power generation curve of a smoky day (September 7th) that includes a short period of cloud cover from 2:00 PM to 3:15 PM. The cloud impact period on power generation is delineated. Furthermore, Fig. 6 depicts the PV power output on cloudy days in early September. Both figures clearly demonstrate that cloud cover results in a sharp reduction in PV power output, which can be easily distinguished from the Wiggle Effect caused by wildfire smoke. Besides the significant difference in PV power output reduction between clouds and wildfire smoke, wildfire smoke can last for days or even weeks and covers large-scale landmass. As mentioned previously, few studies have developed different approaches to quantify the power output reduction caused by wildfire smoke, but none of them considers the rapid power output variation of PV systems due to the Wiggle Effect. Although previous studies have explored diverse methodologies to quantify the reduction in power output caused by wildfire smoke, none of them have taken into account the rapid fluctuations in power output of PV systems resulting from the Wiggle Effect.

There has been extensive research and discourse on solar generation forecasting considering the influence of clouds [40], [41], [42], [43], [44], [45], [46]. A review conducted by the authors in [40] encompassed various solar forecasting techniques with differing time horizons, incorporating the movement of clouds. The paper [41] proposed a method for tracking and predicting cloud motion using ground-based sky images, which can be applied to short-term PV generation forecasting. Another review in [42] evaluated current solar forecasting techniques, including time-series prediction, sky imagers, satellite imaging, numerical weather prediction, and ensemble forecasting. In [43], the authors examined the transient impact of clouds on distribution networks featuring large-scale PV systems. Paper [44] analyzed the impact of clouds on PV systems based on measurements from cloud speed sensors. Additionally, papers [45] and [46] developed short-term solar forecasting methods that considered cloud movement using Artificial Intelligence (AI) and sky images. Furthermore, paper [47] employed statistical numerical models to develop an ultra-short-term cloud forecasting method for solar generation. However, due to the distinct characteristics between cloud and smoke impacts on PV power output, the existing literature on cloud impact cannot be directly applied to analyze the Wiggle Effect in power systems.

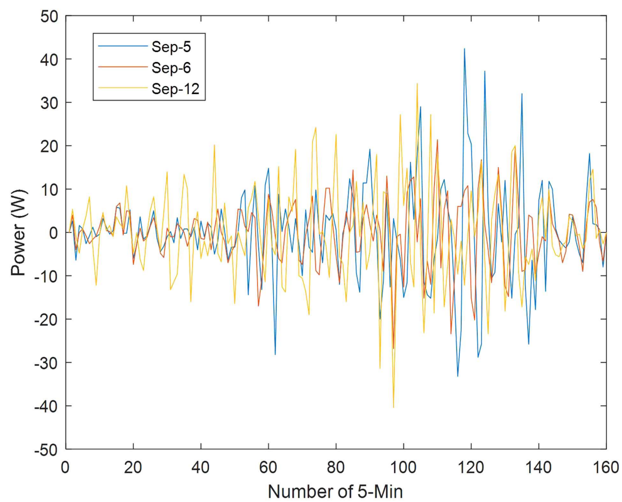

Fig. 7. Wiggle effect on the 3-kW PV system.

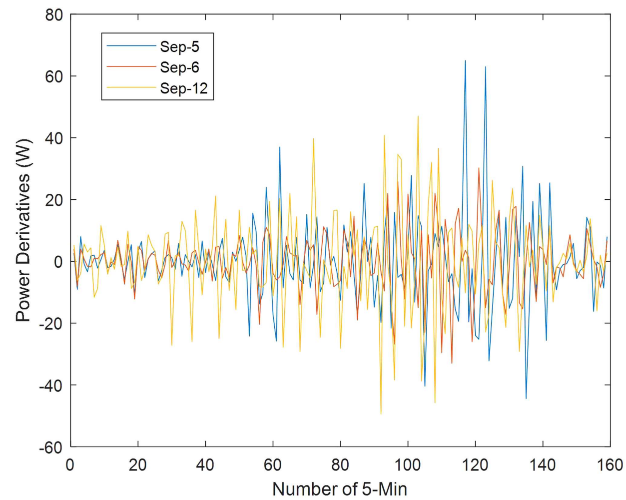

Fig. 8. Derivatives of wiggle effect on the 3-kW PV system.

This research gap poses a potential risk to the stability of power grids with high levels of solar generation and the escalating occurrence of wildfires. Therefore, it is imperative to investigate the Wiggle Effect and comprehensively understand its implications on power system operations.

C. Wiggle Effect Analysis

To understand the Wiggle Effect of wildfire smoke on PV power output, the solar generation deviations during smoky days are extracted using (1)

$$PD(t) = PG_{actual}(t) - PG_{smooth}(t) \quad (1)$$

where *PD* is the PV power output deviation, PG_{actual} is actual power generation during smoky period, and PG_{smooth} is smoothed power generation after using smooth filter. To eliminate the possible power output deviation caused by the panel itself, the power deviation on September 4th (non-smoky and cloudless day) is utilized as the baseline. The wiggle effect for each smoky day is calculated using (2)

$$WE(t) = PD_{smoky}(t) - PD_{Ref}(t) \quad (2)$$

where *WE* is the Wiggle Effect in Watt, PD_{smoky} represents the power output deviation on a smoky day, and PD_{ref} is the power output deviation on a cloudless and non-smoky day. Fig. 7 shows the Wiggle Effect on the 3-kW PV system power output for each smoky day.

In order to assess the impact of the Wiggle Effect on frequency stability, the derivative of the Wiggle Effect is calculated and presented in Fig. 8. The average power derivative of a 3-kW solar system, based on 5-minute data, is approximately 9W. The maximum power derivative observed is 65W, which corresponds to approximately 2.17% of the capacity of the PV system. Thus, in this study, we consider the sudden power generation change of a PV system to be 2.17%, representing the Wiggle Effect induced by wildfire smoke.

III. Wiggle Effect on Frequency Stability

The contemporary power system confronts noteworthy frequency stability challenges arising from decreased system inertia, primarily attributed to the escalating adoption of IBRs [17]. In addition, the proliferation in both the frequency and intensity of wildfires has the potential to further exacerbate the frequency stability predicament encountered by power grids characterized by a substantial integration of PV systems. The existing literature primarily focuses on studying the reduction in PV power generation due to wildfire smoke, overlooking the fluctuations in PV power output caused by the Wiggle Effect, which can impact the frequency stability of the power grid. Therefore, in this section, we calculate the generation deviation resulting from the Wiggle Effect in three major power systems across the United States. Furthermore, we analyze the frequency stability, considering various levels of PV capacities.

A. Power Deviation Analysis

To ensure the frequency stability of power systems, it is crucial to maintain a balance between load and available resources. However, during power system disturbances or outages, this balance is disrupted, resulting in frequency changes that can compromise the stability and reliability of power grids. To assess the frequency deviation induced by the Wiggle Effect, we evaluate power generation deviations at different levels of PV generation. In this study, we focus on two major power systems in the United States: the California Independent System Operator (CAISO) and the Electric Reliability Council of Texas (ERCOT) systems. The total PV capacities in these systems, as reported by the National Renewable Energy Laboratory (NREL) by the end of 2021, are 26.6 GW for CAISO and 10.329 GW for ERCOT [11].

Considering that wildfire smoke can cover a large geographical area, as depicted in Fig. 2, we determine the potential power deviations for CAISO and ERCOT based on the maximum Wiggle Effect observed in the previous section, which corresponds to 2.17% of the total capacity of the PV systems. We calculate

TABLE I
ESTIMATED POWER DEVIATION CAUSED BY THE WIGGLE EFFECCT

ISOs	PV Capacity (GW)	PV Power Supply Deviation (MW)
CAISO	26.6	577
ERCOT	10.329	224

TABLE II
FREQUENCY STABILITY CONTROL MECHANISMS

Control	Ancillary Service	Timeframe
Primary Control	Frequency Response	10-60 Seconds
Secondary Control	Frequency Regulation	1-10 Minutes
Tertiary Control	Imbalance/Reserve	10 Minutes-Hours
Time Control	Time Error Correction	Hours

the estimated power generation deviations resulting from the Wiggle Effect and present them in Table I.

B. Frequency Stability Analysis

The balance between power supply and demand is crucial to maintain the frequency stability of the power grid. Once the mismatch between supply and demand is significant, power system frequency stability could be jeopardized. Currently, various frequency control strategies are applied to maintain the system frequency stability. Based on North America Electric Reliability Cooperation (NERC), the frequency control mainly occurred over a continuum of time using four different types of controls which are primary control, secondary control, tertiary control, and time control shown in Table II [48].

Primary Control, which is interchangeably referred to as Frequency Response, is a mechanism that takes action in the initial seconds after a disturbance in frequency occurs. It's essential to note that Primary Control doesn't restore the frequency to its normal range; instead, it serves the crucial role of stabilizing it. Secondary Control, on the other hand, operates within a timeframe of minutes and is tasked with the function of bringing the frequency back to its nominal value. A widely used form of Secondary Control is Automatic Generation Control (*AGC*). *AGC* is active during the steady state, once the transient effects have subsided. *AGC*'s primary role is to maintain the frequency that has been pre-set by employing Area Control Error (*ACE*) as a tool for balancing authorities. *ACE* is crucial as it serves as the chief input to *AGC*. It is quantified as the megawatt (MW) equivalent adjustment required to align the actual system frequency with the predetermined system frequency value. The mathematical representation to calculate *ACE* is as follows:

$$ACE = -10\beta \left(F_S - F_A\right) \tag{3}$$

where F_s is scheduled frequency, F_A is the actual frequency of the system, and β is system frequency bias. When *ACE* is greater than 0, regulation up (Reg Up) will be applied by the system operator. When *ACE* is less than 0, regulation down (Reg Down) is applied. NERC defines frequency bias as balancing authorities' obligation to provide or absorb energy to stabilize the system frequency, and it is stated in MW/0.1 Hz [48].

$$\beta = -\frac{\Delta P}{\Delta f} \tag{4}$$

where $\Delta f = F_s - F_A$, and ΔP is the power deviation caused by the Wiggle Effect the wildfire smoke. According to the data from NERC, the frequency biases for CAISO and ERCOT are -344.5 MW/0.1 Hz and -789.3 MW/0.1 Hz, respectively [49]. Therefore, the frequency deviation in these two systems can be estimated using $\Delta f = -\Delta P/\beta$ and shown in Table III.

TABLE III
FREQUENCY DEVIATION DUE TO THE WIGGLE EFFECT

Power System	Power Demand Deviation (MW)	Frequency Deviation (Hz)
CAISO	577	0.1676
ERCOT	224	0.0284

TABLE IV
CAPACITY FOR REGULATION SERVICE

Power System	Frequency Deviation (Hz)	Required Reserve Capacity (MW)
CAISO	0.1676	453
ERCOT	0.0284	90

Table III displays the frequency variations as influenced by each system's present frequency bias, along with the estimated deviations in PV power output. The term "*deadband frequency*" refers to the least amount of deviation from the 60 Hz benchmark that must be met before eliciting a response from the governor. At present, the governor frequency deadbands for CAISO and ERCOT are set at 0.036 Hz and 0.017 Hz, respectively, as cited in the reference [50], [51].

It is noteworthy that the frequency deviations caused by the phenomenon known as the 'Wiggle Effect' surpass the deadband thresholds in each of the systems. This implies that the fluctuations induced by the Wiggle Effect are significant enough to prompt a response from the governors in both CAISO and ERCOT systems.

In order to uphold frequency stability while taking into account the impact of the Wiggle Effect on PV power output, each system must allocate sufficient capacity for regulation services. The calculation for determining the necessary capacity for regulation service can be performed using (3). This ensures that the system can effectively counterbalance the fluctuations caused by the Wiggle Effect and maintain stability in frequency.

$$Capacity = (\Delta f - deadband) \times 10 \times -\beta \tag{5}$$

The minimum capacity in each system for regulation service are determined using (3) and shown in Table IV.

Table IV presents the capacity that each system needs to sustain a frequency of 60 Hz. To exemplify these findings, consider CAISO, which has 26.6 GW of installed PV capacity and a frequency bias of -344.5 MW/0.1 Hz. In order to maintain

TABLE V
PV CAPACITY ASSUMPTION

Year	PV Capacity Assumption (GW)	
	California	Texas
2024	33	19
2026	39	28
2028	45	36
2030	50	45
2032	56	54

TABLE VI
FREQUENCY BIAS ASSUMPTION

Year	β (MW/0.1 Hz) Assumption	
	CAISO	ERCOT
2024	-310	-710
2026	-279	-639
2028	-251	-575
2030	-226	-518
2032	-203	-466

TABLE VII
FUTURE POWER DEVIATION

Year	Power Deviation Estimation (MW)	
	CAISO	ERCOT
2024	707	412
2026	846	607
2028	977	781
2030	1085	977
2032	1215	1172

TABLE VIII
ESTIMATED FREQUENCY DEVIATION

Year	Frequency Deviation Δf Forecast (Hz)	
	CAISO	ERCOT
2024	0.2281	0.058
2026	0.3032	0.095
2028	0.3892	0.1358
2023	0.4801	0.1886
2032	0.5985	0.2515

stability in system frequency, factoring in the Wiggle Effect induced by wildfire smoke, CAISO should have a minimum reserve capacity of 491.6 MW.

As the integration of PV systems continues to rise, there is a growing need for reserve capacity with rapid-response capabilities to uphold frequency stability. Consequently, having precise knowledge of the total installed PV capacity and the system's inertia is crucial for the effective operation of the power system in the future.

IV. PREDICTIVE ANALYSIS FOR THE LOW INERTIA TREND

According to the solar industry update from NREL, in the year 2021, CAISO and ERCOT systems saw the addition of 2.984 GW and 4.344 GW in PV capacities, respectively [11]. Theoretically speaking, as the integration of Inverter-Based Resources (IBRs) continues to grow, there will be a corresponding decline in the inertia of power grids. As a result, the settings for frequency bias in power systems are expected to decrease. This section delves into a forward-looking analysis of frequency stability, considering the trend of diminishing inertia coupled with the escalation in PV capacities in the power grids of the future.

To show the possible frequency stability issue with the increasing solar PV capacity and low inertia trending in power grids caused by the Wiggle Effect, CAISO and ERCOT systems are utilized in this study as an example. This study assumes the total PV capacities for each system from 2024 to 2032 shown in Table V. The predicted power deviation and frequency deviation from 2024 to 2032 are derived from this assumption. Additionally, assumptions are made for the frequency bias settings in each system, where a rate of decline by 10% every 2 years is anticipated. This data is presented in Table VI.

To calculate the frequency deviations induced by the Wiggle Effect, considering the assumed parameters for CAISO and ERCOT as displayed in Tables V and VI, the power deviation is ascertained by utilizing 2.17% of the PV capacity, as established in Section II. The results of this calculation are presented in Table VII. This estimation process helps in understanding the potential frequency deviations due to the Wiggle Effect in relation to the parameters and conditions within the CAISO and ERCOT systems.

Table VIII reveals that the CAISO and ERCOT systems may be susceptible to vulnerabilities as PV capacities increase and system inertias decrease. It is evident from the data that the Wiggle Effect has the potential to impact system stability significantly. This highlights the importance of carefully managing and monitoring the integration of PV capacities and the corresponding changes in system inertia to mitigate the risks posed by the Wiggle Effect on the overall stability of the CAISO and ERCOT systems.

To provide a clearer depiction of the potential issues related to frequency stability that may arise due to the Wiggle Effect of wildfire smoke, particularly in the context of increasing PV integration and declining inertia in future power grids, a trend analysis of frequency deviation is conducted. This analysis is based on 2.17% of the total PV capacity and the resulting trends are graphically represented in Fig. 9. Through this visual representation, it is easier to understand and analyze the interplay between the Wiggle Effect, PV penetration, and system inertia, and how these factors can collectively impact the frequency stability in the power grids of the future. As depicted in Fig. 9, as the PV capacity in the power grid increases, it becomes imperative for the power system to have appropriate frequency bias settings in place to maintain frequency stability. Consequently, safeguarding the inertia of power grids becomes a critical factor in ensuring the stability of these grids, especially considering the escalating deployment of IBRs. This highlights the necessity for careful management and monitoring of grid inertia and frequency bias settings to adapt to the changing dynamics brought about by the increasing integration of PV systems.

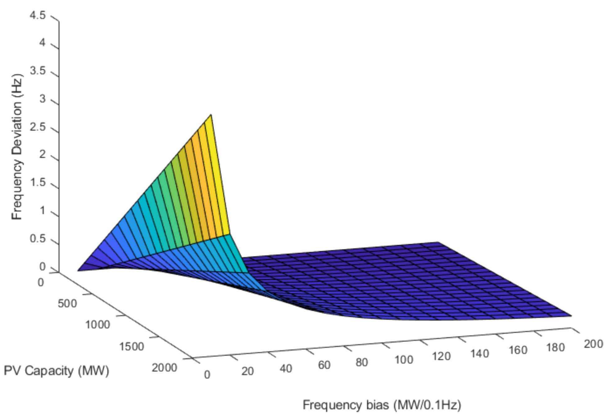

Fig. 9. Frequency stability prediction considering the wiggle effect.

V. Conclusion and Future Works

In this research paper, the "Wiggle Effect" on PV systems caused by wildfire smoke is introduced and analyzed. A predictive analysis for frequency stability is conducted using parameters derived from the CAISO and ERCOT systems. The Wiggle Effect has the potential to jeopardize the stability of power grids without appropriate stability control strategies. This becomes increasingly significant with the rise in PV capacities and the trend towards lower inertia in power systems. This paper represents the first study discussing the impact of the Wiggle Effect on PV systems due to wildfire smoke. By presenting this unique perspective, the paper serves as a valuable resource for power system operators, providing deeper insights into how wildfire smoke can regionally impact the stability of power systems. These insights are essential for informed decision-making and the development of strategies to ensure grid stability.

Future research in this area should explore specific solutions, including advanced control mechanisms, adaptable reserve capacities, and innovative solar cell types, to mitigate the influence of the wiggle effect on power grid frequency stability.

References

[1] San-Miguel-Ayanz, "Forest fires in Europe, Middle East, and North Africa 2020," Publications Office of the European Union, Luxembourg, Eur. Commission, Tech. Rep. JRC126766, 2021.
[2] "2021 international wildfires," Center for Disaster Philanthropy, Oct. 2021. Accessed: Dec. 23, 2021. [Online]. Available: https://disasterphilanthropy.org/disaster/2021-international-wildfires/
[3] "2021 north american wildfire season," Center for Disaster Philanthropy, Dec. 2021. Accessed: Dec. 23, 2021. [Online]. Available: https://disasterphilanthropy.org/disaster/2021-north-american-wildfire-season/
[4] K. Hoover and L. A. Hanson, "Wildfire statistics." [Online]. Available: https://apps.dtic.mil/sti/pdfs/AD1143321.pdf
[5] "Wildland fire summary and statistics annual report," National Interagency Coordination Center, 2022. [Online]. Available: https://www.nifc.gov/sites/default/files/NICC/2-Predictive%20Services/Intelligence/Annual%20Reports/2022/annual_report.2.pdf?mf_ct_campaign=msn-feed&utm_content=syndication
[6] M. Dunleavy, "Declaration of disaster emergency," Alaska, USA, Apr. 1, 2022. [Online]. Available: https://ieeeauthorcenter.ieee.org/wp-content/uploads/IEEE-Reference-Guide.pdf
[7] Alaska Wildland Fire Information, Jul. 2022. Accessed: Sep. 21, 2022. [Online]. Available: https://akfireinfo.com/2022/07/03/alaska-surpasses-2-million-acres-burned/
[8] "Renewables 2021 global status report," Paris, France, 2021. [Online]. Available: https://www.ren21.net/wp-content/uploads/2019/05/GSR2021_Full_Report.pdf
[9] "Renewables 2021," IEA, Paris, France, 2021. [Online]. Available: https://www.iea.org/reports/renewables-2021
[10] V. Ramasamy et al., "U.S. Solar photostatic system and energy storage cost benchmarks, with minimum sustainable price analysis: Q1 2022," NERL, Clean Kilowatts, US DoE solar energy technology office, Sep. 2022. [Online]. Available: https://www.nrel.gov/docs/fy22osti/83586.pdf
[11] D. Feldman, K. Dummit, J. Zuboy, J. Heeter, K. Xu, and R. Margolis, "Spring 2022 solar industry update," Apr. 26, 2022. [Online]. Available: https://www.nrel.gov/docs/fy22osti/82854.pdf
[12] "Fact sheet," Federal Energy Regulatory Commission, Sep. 2022. Accessed: Jun. 24, 2022. [Online]. Available: https://www.ferc.gov/media/ferc-order-no-2222-fact-sheet
[13] "The white house," Apr. 2021. Accessed Sep. 24, 2021. [Online]. Available: https://www.whitehouse.gov/briefing-room/statements-releases/2021/04/22/fact-sheet-president-biden-sets-2030-greenhouse-gas-pollution-reduction-target-aimed-at-creating-good-paying-union-jobs-and-securing-u-s-leadership-on-clean-energy-technologies/
[14] J. Kerry, G. Mccarthy "The long-term strategy of the United States: Pathways to net-zero greenhouse gas emissions by 2050," US Department of State and the US Executive Office of the president, Washington DC, USA, Nov. 2021. [Online]. Available: https://www.whitehouse.gov/wp-content/uploads/2021/10/US-Long-Term-Strategy.pdf
[15] V. Knap, S. K. Chaudhary, D.-I. Stroe, M. Swierczynski, B.-I. Craciun, and R. Teodorescu, "Sizing of an energy storage system for grid inertial response and primary frequency reserve," *IEEE Trans. Power Syst.*, vol. 31, no. 5, pp. 3447–3456, Sep. 2016.
[16] "Inertia: Basic concepts and impacts on the ERCOT grid," ERCOT, Apr. 4, 2018. [Online]. Available: https://www.ercot.com/files/docs/2018/04/04/Inertia_Basic_Concepts_Impacts_On_ERCOT_v0.pdf
[17] K. S. Ratnam, K. Palanisamy, and G. Yang, "Future low-inertia power systems: Requirements, issues, and solutions - A review," *Renewable Sustain. Energy Rev.*, vol. 124, 2020, Art. no. 109773.
[18] Z. Wang, L. Bao, L. Fan, Z. Miao, and S. Shah, "From event data to wind power plant DQ admittance and stability risk assessment," *IEEE Trans. Power Syst.*, vol. 37, no. 6, pp. 4400–4408, Nov. 2022.
[19] D. Sun, H. Liu, and M. Gong, "A stability analysis tool for bulk power systems using black-box models of inverter-based resources," in *Proc. IEEE Ind. Appl. Soc. Annu. Meeting*, 2022, pp. 1–6.
[20] A. M. Jobayer, M. R. Chowdhury, L. Zhao, A. Papasani, Y. Zhou, and W.-J. Lee, "Impact of societal events on frequency stability considering LED TVs in low inertia trending power systems," *IEEE Trans. Ind. Appl.*, vol. 57, no. 6, pp. 5649–5657, Nov./Dec. 2021, doi: 10.1109/TIA.2021.3106874.
[21] H. Bevrani, A. Ghosh, and G. Ledwich, "Renewable energy sources and frequency regulation: Survey and new perspectives," *IET Renewable Power Gener.*, vol. 4, no. 5, pp. 438–457, 2010.
[22] U. Bose, S. K. Chattopadhyay, C. Chakraborty, and B. Pal, "A novel method of frequency regulation in microgrid," *IEEE Trans. Ind. Appl.*, vol. 55, no. 1, pp. 111–121, Jan./Feb. 2019.
[23] X. Liang, "Emerging power quality challenges due to integration of renewable energy sources," *IEEE Trans. Ind. Appl.*, vol. 53, no. 2, pp. 855–866, Mar./Apr. 2017.
[24] Y. Liu, S. You, and Y. Liu, "Study of wind and PV frequency control in U.S. power grids—EI and TI case studies," *IEEE Power Energy Technol. Syst. J.*, vol. 4, no. 3, pp. 65–73, Sep. 2017.
[25] N. Soni, S. Doolla, and M. C. Chandorkar, "Improvement of transient response in microgrids using virtual inertia," *IEEE Trans. Power Del.*, vol. 28, no. 3, pp. 1830–1838, Jul. 2013.
[26] "Fire and smoke map," AirNow, 2022. Accessed: Sep. 12, 2022. [Online]. Available: https://fire.airnow.gov/
[27] A. Umunnakwe, M. Parvania, H. Nguyen, and J. D. Horel, "Data-driven spatio-temporal analysis of wildfire risk to power systems operation," *IET Gener., Transmiss. Distrib.*, vol. 16, no. 13, pp. 2531–2546, 2022.
[28] I. N. Sokolik, A. J. Soja, P. J. DeMott, and D. Winker, "Progress and challenges in quantifying wildfire smoke emissions, their properties, transport, and atmospheric impacts," *J. Geophysical Res.: Atmospheres*, vol. 124, pp. 13005–13025, 2019.
[29] A. Vicente et al., "Emission factors and detailed chemical composition of smoke particles from the 2010 wildfire season," *Atmospheric Environ.*, vol. 71, pp. 295–303, 2013.

[30] U. Makkonen, H. Hellén, P. Anttila, and M. Ferm, "Size distribution and chemical composition of airborne particles in south-eastern Finland during different seasons and wildfire episodes in 2006," *Sci. Total Environ.*, vol. 408, pp. 644–651, 2010.

[31] S. York, "U.S. Information Administration," Sep. 2020. Accessed: Sep. 23 2021. [Online]. Available: https://www.eia.gov/todayinenergy/detail.php?id=45336

[32] M. Perry and A. Troccoli, "Impact of a fire burn on solar irradiance and PV power," *Sol. Energy*, vol. 114, pp. 167–173, 2015.

[33] A. J. Ali, L. Zhao, M. H. Kapourchali, and W.-J. Lee, "Development of quantification method for wildfire smoke impact on photovoltaic system," in *Proc. IEEE/IAS 59th Ind. Commercial Power Syst. Tech. Conf.*, 2023, pp. 1–10, doi: 10.1109/ICPS57144.2023.10142101.

[34] D. L. Donaldson, D. M. Piper, and D. Jayaweera, "Temporal solar photovoltaic generation capacity reduction from wildfire smoke," *IEEE Access*, vol. 9, pp. 79841–79852, 2021.

[35] A. Z. Bertoletti, T. Phan, and J. C. do Prado, "Wildfire smoke, air quality, and renewable energy—Examining the impacts of the 2020 wildfire season in Washington State," *Sustainability*, vol. 14, no. 15, 2022, Art. no. 9037.

[36] S. D. Gilletly, N. D. Jackson, and A. Staid, "Quantifying wildfire-induced impacts to photovoltaic energy production in the western United States," in *Proc. IEEE 48th Photovoltaic Specialists Conf.*, 2021, pp. 1619–1625.

[37] A. J. Ali, L. Zhao, and M. H. Kapourchali, "Data-driven-based analysis and modeling for the impact of wildfire smoke on PV systems," *IEEE Trans. Ind. Appl.*, doi: 10.1109/TIA.2023.3292807.

[38] M. Cai, C. Lin, V. Ravi, Y. Zhang, C. Lu, and M. Sengupta, "Final technical reprot: Impact of wildfires on solar generation, reserves, and energy prices," NREL, Jul. 2023. Accessed: October 10, 2023. [Online]. Available: https://www.nrel.gov/docs/fy23osti/86640.pdf

[39] "Smoky fires rage in the northwest," Sep. 2022. Accessed: Sep. 27, 2022. [Online]. Available: https://earthobservatory.nasa.gov/images/150328/smoky-fires-rage-in-the-northwest

[40] T. Kato, "Integration of distributed energy resources in power systems," in *Prediction of Photovoltaic Power Generation Output and Network Operation*. Amsterdam, The Netherlands: Elsevier, 2016, pp. 78–106.

[41] D. M. L. H. Dissawa, M. P. B. Ekanayake, G. M. R. I. Godaliyadda, J. B. Ekanayake, and A. P. Agalgaonkar, "Cloud motion tracking for short-term on-site cloud coverage prediction," in *Proc. 17th Int. Conf. Adv. ICT Emerg. Regions*, 2017, pp. 1–6.

[42] A. Tuohy et al., "Solar forecasting: Methods, challenges, and performance," *IEEE Power Energy Mag.*, vol. 13, no. 6, pp. 50–59, Nov./Dec. 2015.

[43] J. Krata, T. K. Saha, and R. Yan, "Large scale photovoltaic system and its impact on distribution network in transient cloud conditions," in *Proc. IEEE Power Energy Soc. Gen. Meeting*, 2015, pp. 1–5.

[44] K. Lappalainen and J. Kleissl, "Analysis of the cloud enhancement phenomenon and its effects on photovoltaic generators based on cloud speed sensor measurements," *J. Renewable Sustain. Energy*, vol. 12, 2020, Art. no. 043502.

[45] Z. Zhen et al., "Deep learning based surface irradiance mapping model for solar PV power forecasting using sky image," *IEEE Trans. Ind. Appl.*, vol. 56, no. 4, pp. 3385–3396, Jul./Aug. 2020.

[46] X. Meng, F. Gao, T. Xu, K. Zhou, W. Li, and Q. Wu, "Inverter-data-driven second-level power forecasting for photovoltaic power plant," *IEEE Trans. Ind. Electron.*, vol. 68, no. 8, pp. 7034–7044, Aug. 2021.

[47] Y. Huang, J. Lu, C. Liu, X. Xu, W. Wang, and X. Zhou, "Comparative study of power forecasting methods for PV stations," in *Proc. Int. Conf. Power Syst. Technol.*, 2010, pp. 1–6.

[48] "Balancing and frequency control reference document," NERC, Atlanta, GA, USA, May 11, 2021. [Online]. Available: https://www.nerc.com/comm/OC/ReferenceDocumentsDL/Reference_Document_NERC_Balancing_and_Frequency_Control.pdf

[49] "OY_2022_Frequency_Bias_Annual_Calculations," Jun. 2022. [Online]. Available: https://www.nerc.com/comm/OC/RS%20Landing%20Page%20DL/Frequency%20Response%20Standard%20Resources/OY_2022_Frequency_Bias_Annual_Calculations_REVISION_4.26.22.pdf

[50] *BAL-003-2 Frequency Response Obligation Allocation and Minimum Frequency Bias Settings for Operating Year 2022*, Standard BAL-003-2, NERC, Atlanta, Georgia, 2022.

[51] A. J. Ali, L. Zhao, M. H. Kapourchali, and W.-J. Lee, "The wiggle effect of wildfire smoke on PV systems and frequency stability analysis for low-inertia power grids," in *Proc. IEEE/IAS 59th Ind. Commercial Power Syst. Tech. Conf.*, 2023, pp. 1–8, doi: 10.1109/ICPS57144.2023.10142096.